PROGRESS
IN COLOR, COLORANTS AND COATINGS

available online @ www.pccc.icrc.ac.ir
Prog. Color Colorants Coat. 8(2015), 47-57

Ministry of Science, Research and Technology
Institute for Color Science and Technology

Degradation of C. I. Basic Blue 41 Using Modified TiO_2 Nanocomposite in a Rectangular Semibatch Photoreactor

S. Mohammadi-Aghdam*[1] and M. E. Olya[2]

[1] Assistant Professor, Department of Chemistry, Payame Noor University, P. O. Box: 19395-3697, Tehran, Iran.

[2] Assistant Professor, Department of Environmental Research, Institute for Color Science and Technology, P. O. Box:16765-654, Tehran, Iran.

ARTICLE INFO

Article history:
Received: 05-08-2013
Final Revised: 18-05-2014
Accepted: 26-08-2014
Available online: 26-08-2014

Keywords:
Advanced oxidation processes
TiO_2nano composite film
chemical oxygen demand

ABSTRACT

The aim of this work was to investigate the effect of operational parameters on the photocatalytic degradation efficiency of a solution containing C. I. Basic Blue 41 in a recirculated rectangular photoreactor (irradiated with a UV light TiO_2 nano composite film was prepared via sol-gel dip coating method. The films were characterized by X-ray diffraction, transmission electron microscopy, scanning electron microscopy and coating thickness gauge. Initial concentration of Basic Blue 41 (10-50 mg L^{-1}), flow rate (6-15 L h^{-1}) and temperature (20-40 ºC) were the variables that mostly influenced the degradation efficiency. The results showed that the removal efficiency decreases by increasing the initial concentration and flow rate, however it increases when the temperature increases. To monitor the mineralization of Basic Blue 41, chemical oxygen demand measurements and UV-Vis analyses changes were carried out during the UV/TiO_2 process. The results indicated 92.943% mineralization of 25 mg L^{-1} dye after 2h of UV irradiation. Prog. Color Colorants Coat. 8(2015), 47-57 © Institute for Color Science and Technology.

1. Introduction

During the last two decades, dyes pollutants and their removal from textile industry before discharge has become one of the most significant global Problems [1, 2]. Among various kinds of dyes, azo dyes are utilized more than other ones in textile industries, because they are highly colorful and stable against light and washing. Azo dyes have at least one –N=N– chromophore in their structure, hence they are harmful and should be treated before use [1, 3]. Several common techniques of wastewater treatment like coagulation, electrocoagulation, precipitation adsorption on activated carbon and filtration have been

---

*Corresponding author: *s_mohammadi@iau-tnb.ac.ir* demonstrated in previous studies. But they are often very costly methods and ineffective for complete degradation of some disobedient organic dyes or only transfer the contaminant from one phase to another [4, 5]. Advanced oxidation processes (AOPs) with semiconductor photocatalysis have been developed in recent literatures as alternative for destruction of dyes and non-biodegradable organic compounds by generating reactive species such as $O_2^{\cdot-}$, $HO_2^{\cdot-}$, $OH^{\cdot}$ and electron-hole pairs (e^-/h^+) [6]. Of the many different photocatalysts, TiO_2 has been the most widely studied and used in many application because of its strong oxidizing abilities [7], long durability, non-toxicity, low-cost and biocompatibility [8]. A photocatalyst can be used in two forms: suspended in aqueous solution or immobilized onto a stable and inert substrate [9]. Despite several benefits for slurry systems, there is a significant drawback i.e.; the need to separate TiO_2 nanoparticles after photocatalytic reaction and their reuse [10]. Different materials such as glass [11], mesoporous clays, zeolite [12], polymeric materials [13], non-woven paper [14], sackcloth fiber [15], and carbon nanotube [16] have already been utilized as substrate for TiO_2 to overcome this problem. The aim of this work is to investigate the effect of operational parameters including initial concentration of BB41, flow rate (FR) and temperature on the photocatalytic degradation efficiency of a solution containing Basic Blue 41 (BB41) in a semibatch rectangular reactor with immobilized mesoporous TiO_2 nanocomposite films.

2. Experimental

2.1. Materials

BB41 [1-Amino-6-methoxybenzotiazole] was purchased from Ciba Co (Iran). Figure 1 illustrates some characteristics of BB41. The following components were used for the preparation of TiO_2 nanocomposite sol. Titanium tetraisopropoxide, TTIP ($Ti(OCH(CH_3)_2)_4$, purity > 98%), as a titanium precursor [11-18], Isopropanol, IPA ($(CH_3)_2CHOH$, absolute; ≥99.8%) as a solvent [19], Acetylacetone, AcAc ($(CH_3(CO)CH_2(CO)CH_3)$ as the stabilizer [11, 12, 14-16, 18, 20], Hydrogen peroxide, H_2O_2, 30 wt.% as the oxidant [21], Degussa P25 TiO_2 nano powders (average primary particle size around 30 nm, purity > 97% and 80:20 anatase to rutile ratio) as the filler for increasing the surface area of as-prepared photocatalyst [17-20] and Deionized water, H_2O for gelation [21, 22]. All the chemicals except Degussa P25 powders were of analytical grade from Merck and used without further treatment.

2.2. Preparation of TiO_2 nanocomposite films

TTIP (5 mL), AcAc (3.5 mL) and IPA (10 mL) were added in sequence into a pyrex reactor under constant stirring for 15min, then 20 mL deionized water was added to the mixture and stirred for 20 min at room temperature. The prepared suspension containing titanium hydroxide, i.e., $Ti(OH)_4$ was filtered by vacuum distillation and washed with deionized water two times to yield a white paste. H_2O_2 (20-30 mL), deionized water (100 mL) and Polyethylene glycole, PEG (0.3 g from an aqueous solution of PEG 10 wt. %) were added step by step and agitated for 40 min to form a yellowish titanium peroxide sol. After that it was left 12 hr. at room temperature to complete hydrolysis reaction and obtain a sol with good viscosity.

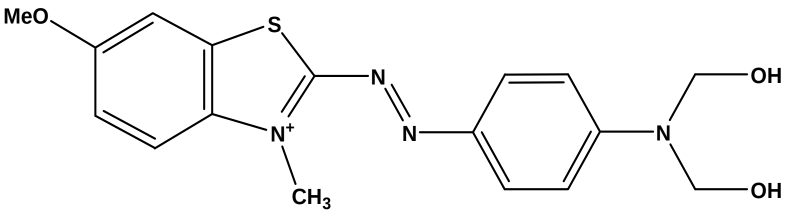

Figure 1: Chemical structure of BB41.

Finally, 10 gr L^{-1} TiO_2 nano powder was slowly added to TiO_2 sol under vigorous stirring to avoid the formation of larger titania agglomerates. Before dip coating the glass plates with dimensions of 400 mm×45 mm×3 mm were carefully washed. Then they were dipped into the sol at a rate of 1m ms^{-1}, and kept for 60 min, and then withdrawn from the sol at same rate. Afterwards, all substrates were first dried at 100 *ºC* for 60 min, then the temperature of the oven was increased at a ramp rate of 5 *ºC* min^{-1} to 500 *ºC* and held for 30 min [23]. Finally, the films were cooled down at room temperature. Dip coating process was carried out three times to generate a three ply film with high adherence.

2.3. Photoreactor and light source

All experiments were performed in a homemade rectangular semibatch-photoreactor (400 mm×150 mm×150 mm) which was consisted of a Pyrex reactor with a high-pressure mercury lamp (15 W, UV-C, manufactured by Osram) encircled by a quartz tube (with outer and inner diameter of 32 and 30 mm, respectively) at the center of it, and TiO_2 films which were placed in the inner wall of reactor (Figure 2).

2.4. Dye dygradation

In each set-up prior to irradiation, 1200 mL of BB41 solution with a desired initial concentration over the catalyst was circulated by a water pump (PASSEO QC, 8 W, $Q_{MAX} = 650$ L h^{-1}) located below the reactor in the dark for 30 min to obtain an adsorption-desorption equilibrium. After adjusting the flow rate and temperature, the lamp was switched on to start the reaction. Sampling was carried out at regular time intervals during irradiation and the samples were analyzed by a double beam UV- Vis spectrophotometer (VARIAN, CARY 100 BIO) to measure the concentration of dye between 200.0-800.0 nm. The removal percentage as a function of time is calculated by equation (3):

$$\%\text{Dye removal}= \frac{C_0 - C_t}{C_0} \qquad (3)$$

where C_0 is the initial concentration of BB41 and C_t represents the absorbance of dye at time t.

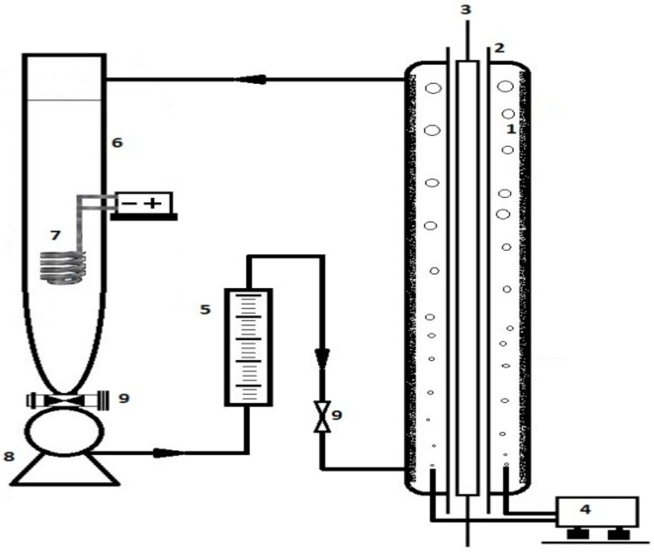

Figure 2: Experimental setup for the photocatalytic degradation of BB41: (1) TiO_2 nano-photocatalyst film; (2) Pyrex reactor; (3) Quartz sleeve with a central UV lamp; (4) Aeration pump; (5) Flow meter; (6) Solution tank; (7) digital heater-thermometer; (8) Water pump; (9) Control value.

3. Results and discussion

3.1. Structural analysis

It can be observed from Figure 3a that the nano composite film has polycrystalline structure. It was confirmed by X-ray diffraction (XRD) peak at 2θ = 25.4° for anatase, and 2θ = 27.3° for rutile. The average crystallite size and the percentage of the anatase phase were calculated by equations 1 and 2, respectively [21, 24, 25]:

$$D=\frac{k\lambda}{\beta\cos\theta} \tag{1}$$

$$\%X=\frac{100}{\left[1+0.8\frac{I_A}{I_R}\right]} \tag{2}$$

where D is the crystallite size, k is a constant equal to 0.94, λ is the wavelength of incident light (0.154 nm), β is the full width at half of the maximum peak height (FWHM) in radians, θ is diffraction angle, x the weight percentage of the anatase phase, I_A and I_R are the maximum peak intensity of anatase and rutile phases, respectively. The results show that the crystallite size obtained from the well-known Debye-Scherrer's equation (equation 1) is 34 nm and the anatase to rutile ratio is 88/12. It is reported that a nano photocatalyst with a mixture of anatase and rutile has a higher photoreactivity than anatase or rutile alone [18].

The grain size of TiO_2 nanocomposite was investigated by Transmission Electron Microscopy (TEM). Figure 3b shows that the majority of TiO_2 nanocomposite is consisted of particles of 30 to 40 nm, which is consistent with the XRD result. The results have summarized in Table 1. Film morphology was investigated by Scanning Electron Microscopy (SEM). Figure 3c shows that TiO_2 nanocomposite is well-immobilized on the glass substrate. Thickness measurement of the film was done with a needle coating thickness gauge with medium scan speed of 25s and resolution of 5000 lm/sample. As shown in Figure 3d, the maximum thickness of the film was about 252.9 nm.

Table 1: The percentage of anatase phase and TiO_2 crystallite size (nm) obtained from Debye-Scherrer's equation and TEM image.

Percentage of anatase phase	Crystallite size (nm)	TEM (nm)
88	34	30-40

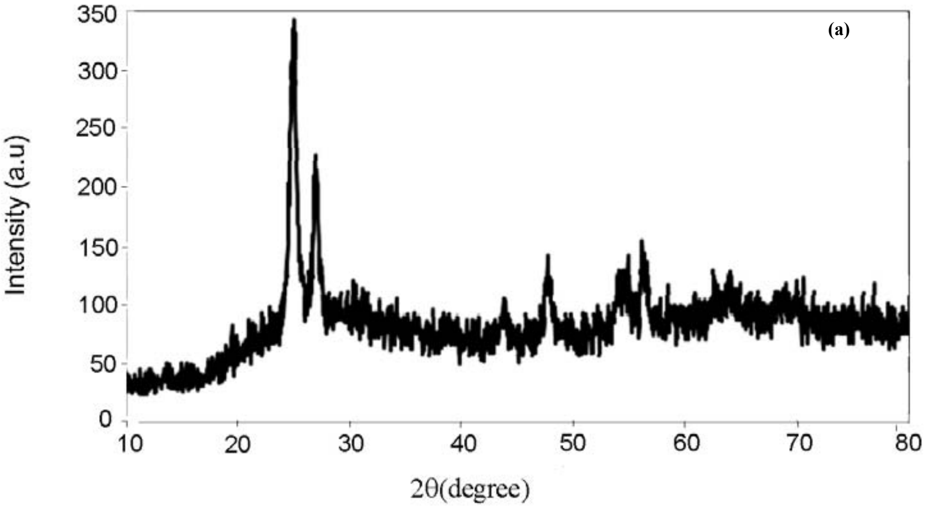

Figure 3: Applied TiO_2 nanocomposite film: (a) XRD pattern, (b) TEM image, (c) SEM image, and (d) Thickness spectra.

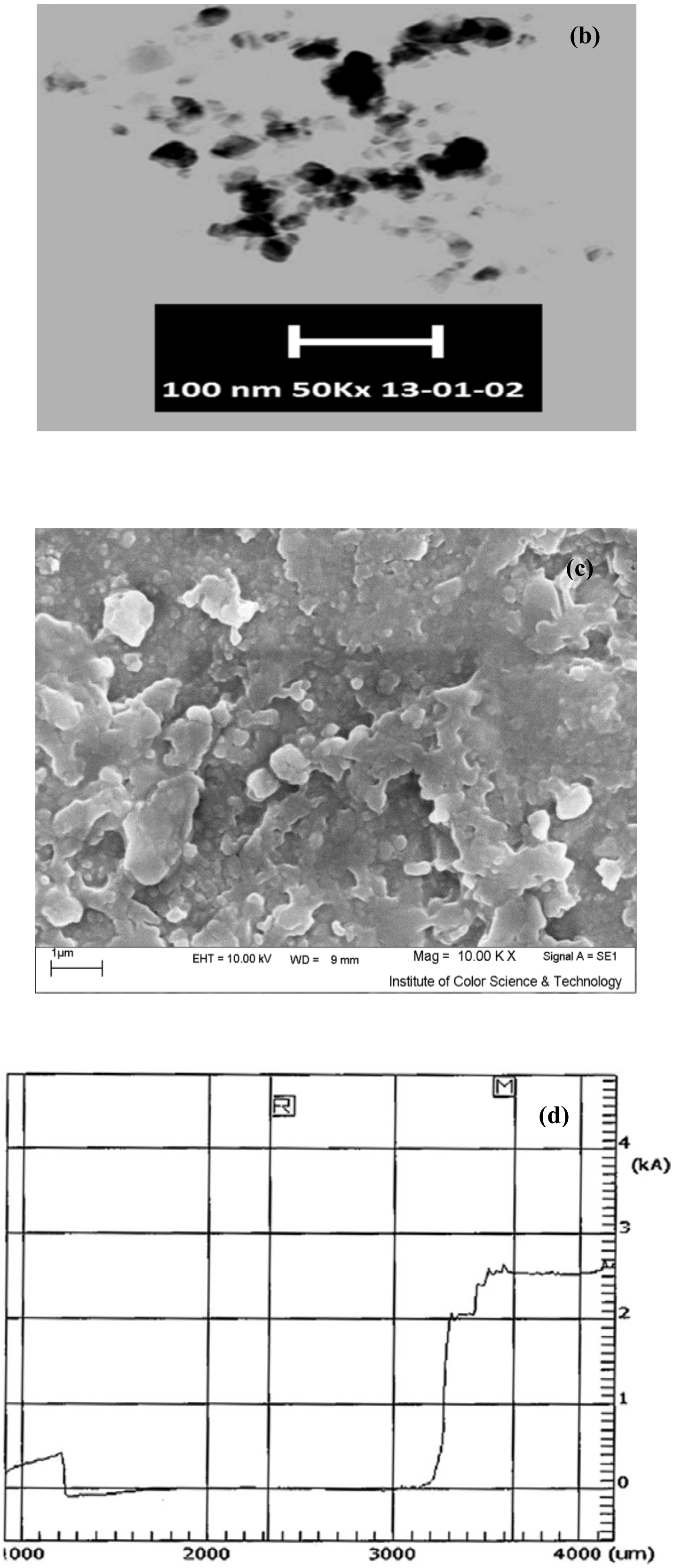

Figure 3: Continued.

3.2. The effect of initial dye concentration

The effect of initial dye concentration on the degradation efficiency was investigated by varying the dye concentrations in the range of 10-50 mg L^{-1} at solution actual pH. The results are shown in Figure 4. It can be seen that with increasing the initial dye concentration, the removal efficiency of BB41 decreases. The presumed reason is that when the initial dye concentration increases, more and more interference would be provided which could prevent further degradation. As a result all of the active sites on the surface of photocatalyst are occupied by dye molecules, so no site will be available for further concentrations [26, 27].

3.3. The effect of flow rate

The removal efficiency versus irradiation time at different flow rates is presented in Figure 5. The results indicate a slight improvement in decolorization efficiency with decreasing flow rate from 15 to 6 L h^{-1} Maximum degradations of 98.7%, 92.94%, 86.68% and 81.35% were obtained for the flow rates of 6, 9, 12 and 15 L h^{-1}, respectively. It can be attributed to the increasing of residence time of the dye molecules beside photocatalyst with decreasing the system turbulence. A similar behavior has been reported by other investigators [28, 29].

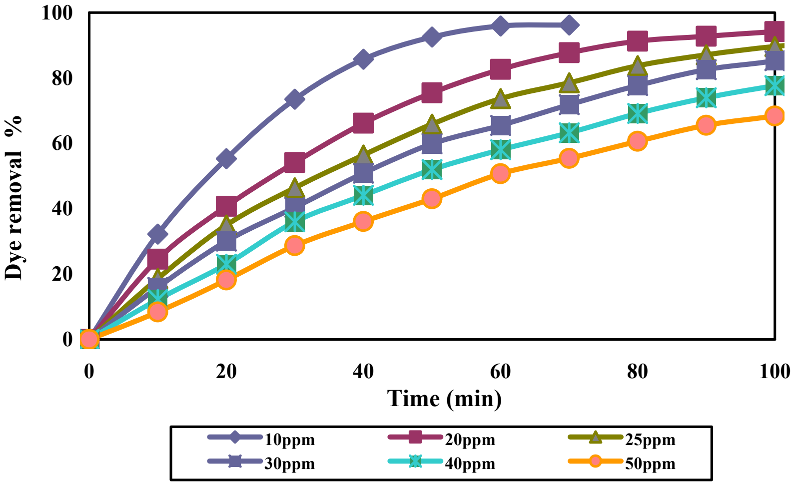

Figure 4: The effect of initial dye concentration on degradation efficiency, T= 298 K and FR= 9 L h^{-1}.

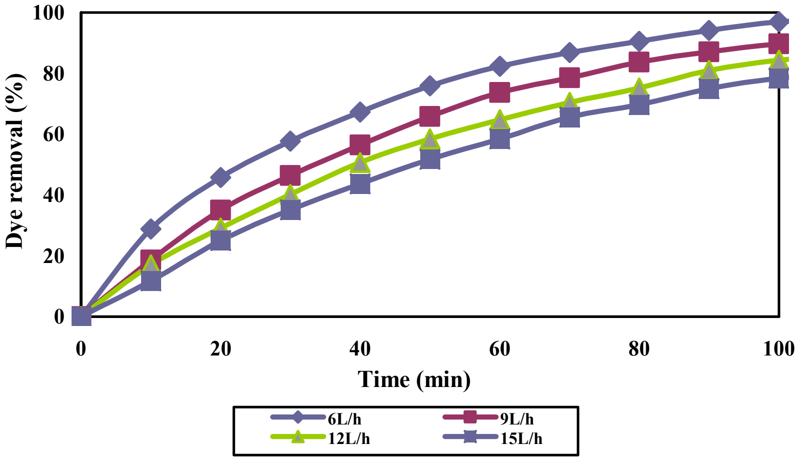

Figure 5: The effect of flow rate on degradation efficiency, $[BB41]_0$ = 25 mg L^{-1} and T= 298 K.

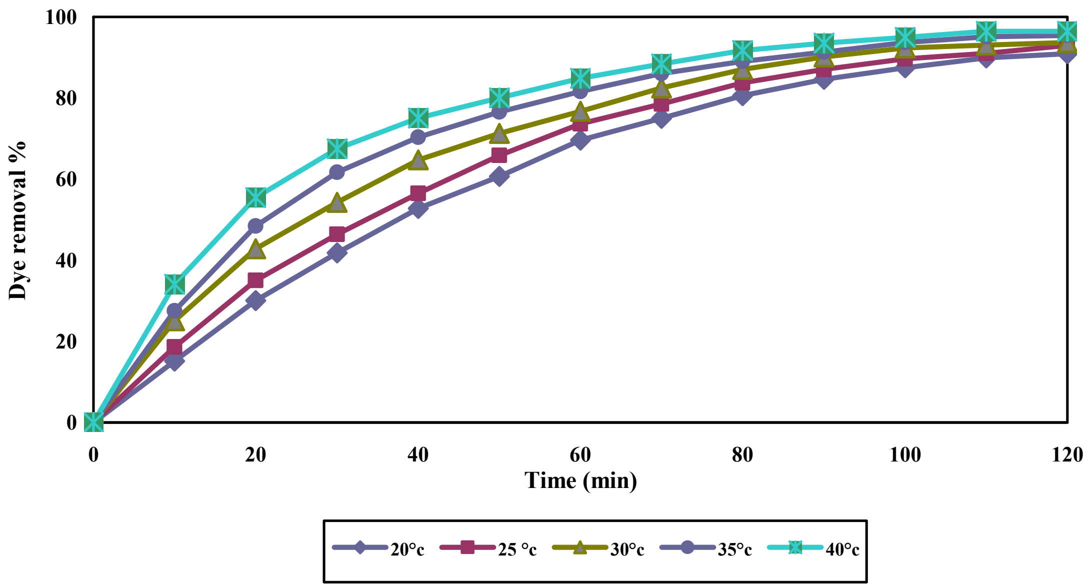

Figure 6: The effect of temperature on degradation efficiency, $[BB41]_0$ = 25 mgL^{-1} and FR= 9 Lh^{-1}.

3.4. The effect of temperature

The photocatalytic degradation reaction rate, similar to any other chemical reaction rates, increases with temperature rise. As shown in Figure 6, when the temperature increases (20-40 °C), the efficiency of BB41 removal increases by about 10%. In fact, as the temperature increases, the formation of e^-/h^+ occurs faster, hence the removal efficiency increases. On the other hand, by increasing the temperature up to 45 ºC, the solubility of oxygen in water decreases which is not advantageous. Moreover, higher temperatures will cause evaporation of solution during the experiment [30].

3.5. UV-Vis spectra

The changes in the UV-Vis absorption spectra of BB41 solutions as a function of irradiation time for photocatalytic degradation of 25 mg L^{-1} of solution are shown in Figure 7. The decline trend of maximum peaks at λ_{max}=607nm indicates a rapid degradation of azo dye from the azo bond (–N=N–) as the most active site for the oxidative attack [31]. As can be seen from Figure 7, almost 93% of the dye has been eliminated in the presence of TiO_2 nanocomposite films.

3.6. Chemical Oxygen Demand (COD) measurement

COD values have been related to the total concentration of organics in the solution [12]. The decrease of COD as a function of irradiation time is shown in Figure 8. It is evident that final COD dosage in outlet stream of photoreactor is significantly low. Also this results show that the outlet stream from photoreactor is considerably mineralized, which is in agreement with the UV-Vis trend. The remaining COD in the final steam could be due to the stable intermediates which are not any more degradable by UV/TiO_2 nanocomposite process [32, 33].

3.7. Kinetics study

Several experimental results [34, 35] indicate that heterogeneous photocatalytic decolorization and degradation of various dyes are well described by a pseudo-first-order kinetic for diluted solutions. The photocatalyticdegradation of BB41 by UV/TiO_2 nanocomposite process follows pseudo-first-order kinetics.

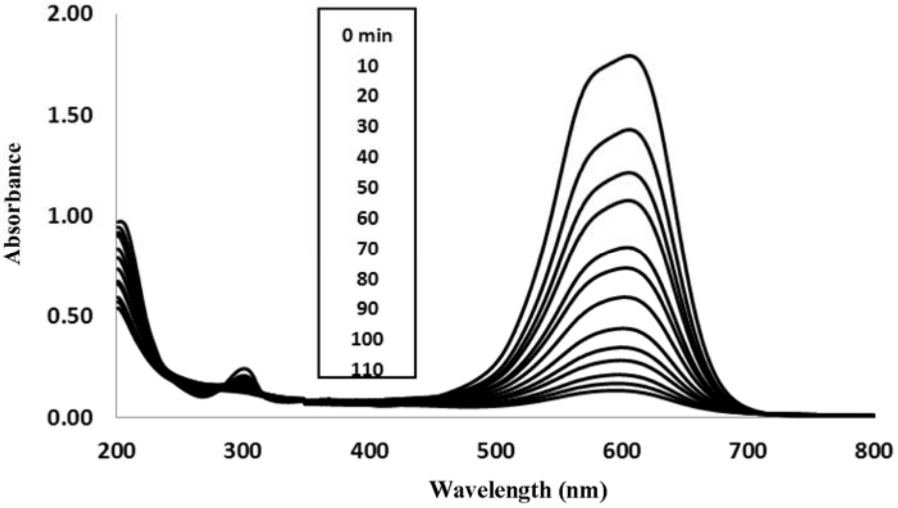

Figure 7: UV- Vis spectra changes of BB41 during the photocatalytic process at different irradiation times; $[BB41]_0$ = 25 mg L^{-1}, T = 298 K natural pH and FR = 9 L h^{-1}.

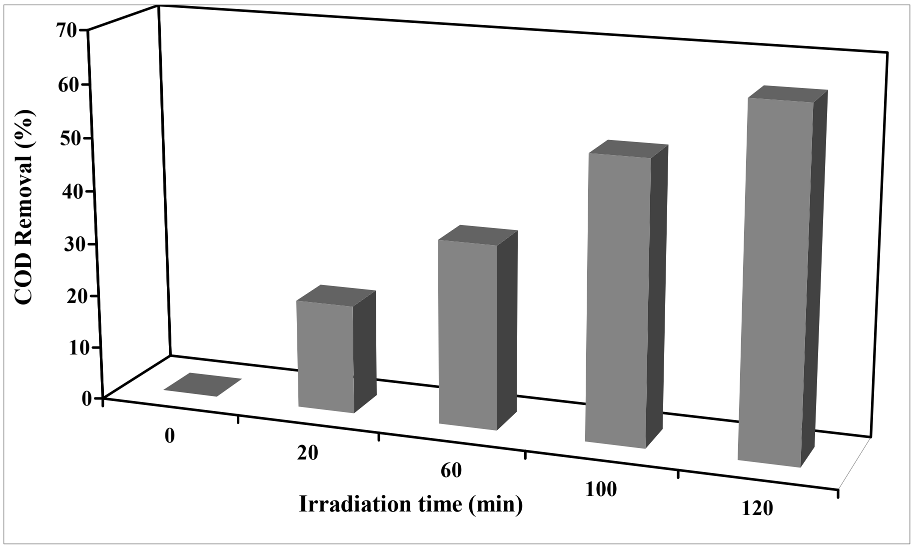

Figure 8: COD removal of BB41aqueous solution during the UV/TiO_2 process $[BB41]_0$ = 25 mg L^{-1}, T= 298K, natural pH and FR =9 L h^{-1}.

At low initial dye concentration the rate expression is given by equation 4.

$$Ln\frac{C}{C_0} = -kt \tag{4}$$

where C_0 and C are initial dye concentration and dye concentration at time *t* (min) respectively, *t* is irradiation time (min) and *k* is the rate constant (min^{-1}). The plot of *Ln C/C₀* versus time for the dye was linear (Figure 9) which can be approximated as pseudo-first-order kinetic model. Straight lines with correlation coefficients of more than 0.99 proved the suggested model. Also apparent rate constant for degradation of BB41 is evaluated through the linear regression of $Ln\ C/C_0$ versus *t*. Figure10 shows the pseudo-first-order reaction rate constants against time. It shows that the apparent rate constant slightly decreases with an increase in the initial amount of BB41 from 10 to 50 mg L^{-1}. Similar results for the photocatalytic oxidation of BB41 are also obtained in other investigations [34, 35].

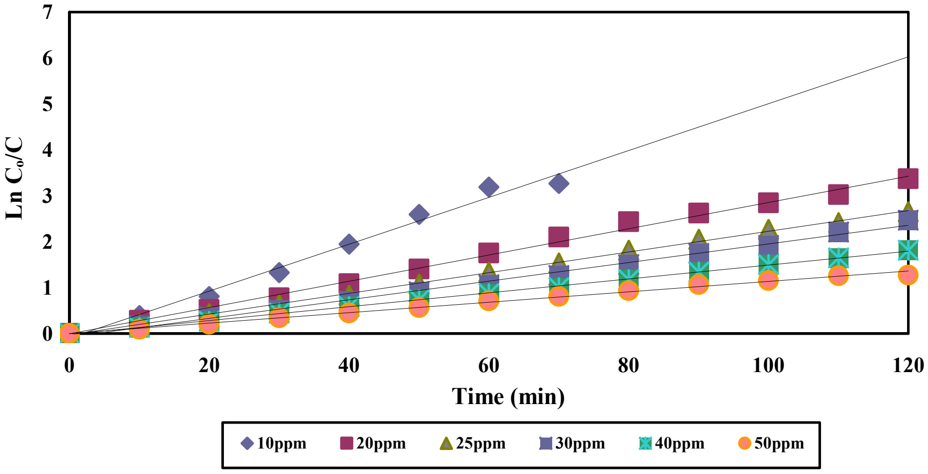

Figure 9: The effect of initial dye concentration on degradation efficiency, T= 298 K and FR= 9 L h^{-1}.

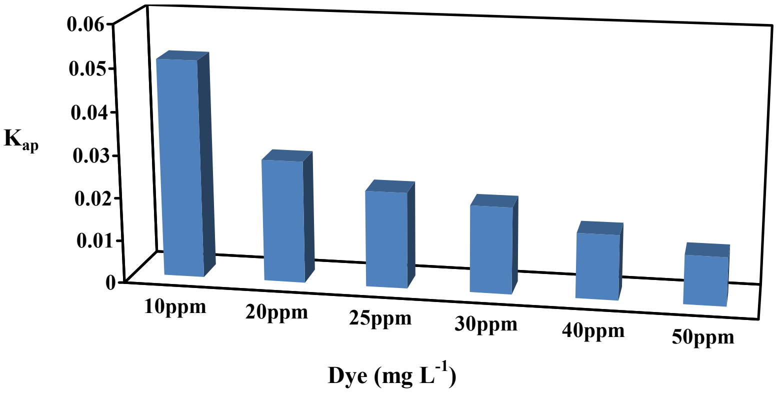

Figure 10: The pseudo-first-order reaction rate constants against time.

4. Conclusions

In this study, photocatalytic degradation of BB41 using immobilized TiO_2 nanocomposite as a photocatalyst in a recirculated rectangular photoreactor (irradiated with a UV light) was performed. The effect of operational parameters such as initial BB41 content, flow rate and temperature were investigated on the removal rate of BB41. The results showed that the removal efficiency decreases by increasing the initial concentration and flow rate, however it increases with the temperature. The removal rate follows a pseudo-first order kinetic with respect to BB41 concentration which decreases with increasing the initial concentration of the dye. The results indicated 92.943% mineralization of 25 mg L^{-1} dye after 2h of UV irradiation.

Acknowledgements

The authors thank the Department of Chemistry, Faculty of Science, Mahabad Branch, Payame Noor University, Mahabad, Iran, and Iranian Nano Technology Initiative Council for financial and other supports.

5. References

1. S. Mohammadi-Aghdam, R. Marandi, M. E. Olya, and A. A. Mehrdad Sharif, Kinetic modeling of BB41 photocatalytic treatment in a semibatch flow photoreactor using a nano composite film, *J Saudi Chem Soc.*, 18(2014), 317-326.

2. N. Modirshahla, M. A. Behnajady, and S. Mohammadi-Aghdam, Investigation of the effect of different electrodes and their connections on the removal efficiency of 4-nitrophenol from aqueous solution by electrocoagulation, *J. Hazard. Mater.,* 154(2008), 778-786.
3. M. E. Olya, A. Pirkarami, M. Soleimani, and N. Y. Limaee, Decolorization of acid dye useing sono-Based processes: sonoelectrochemical, sonophotoelectro-chemical and sonophotoelectro-catalysis, *Prog. Color Colorants Coat.,* 7(2014), 105-120.
4. U. I. Gaya and A. H. Abdullah, Heterogeneous photocatalytic degradation of organic contaminants over titanium dioxide: A review of fundamentals, progress and problems, *J. Photochem. Photobiol., C,* 9(2008), 1-12.
5. A. Mahyar and A. R. Amani-Ghadim, Influence of solvent type on the characteristics and photocatalytic activity of TiO_2 nanoparticles prepared by the sol-gel method, *Micro Nano Lett,* 6(2011), 244-248.
6. A. Fujishima, T. N. Rao, and D. A. Tryk, Titanium dioxide photocatalysis, *J. Photochem. Photobiol., C,* 1(2000), 1-21.
7. Y. Nosaka, M. Nakamura, and T. Hirakawa, Behavior of superoxide radicals formed on TiO_2 powder photocatalysts studied by a chemiluminescent probe method, *Phys. Chem. Chem. Phys.,* 4(2002), 1088-1092.
8. K. Nakata and A. Fujishima, TiO_2 photocatalysis: Design and applications, *J. Photochem. Photobiol., C,* 13(2012), 169-189.
9. S. Šegota, L. Ćurković, D. Ljubas, V. Svetličić, I. F. Houra, and N. Tomašić, Synthesis, characterization and photocatalytic properties of sol–gel TiO_2 films, *Ceram. Int.,* 37(2011), 1153-1160.
10. N. Sasirekha, B. Rajesh, and Y. W. Chen, Synthesis of TiO_2 sol in a neutral solution using $TiCl_4$ as a precursor and H_2O_2 as an oxidizing agent, *Thin Solid Films,* 518(2009), 43-48.
11. Y. Chen, E. Stathatos, and D. D. Dionysiou, Microstructure characterization and photocatalytic activity of mesoporous TiO_2 films with ultrafine anatase nanocrystallites, *Surf. Coat. Technol.,* 202(2008), 1944-1950.
12. E. C. Ilinoiu, R. Pode, F. Manea, L. A. Colar, A. Jakab, C. Orha, et al., Photocatalytic activity of a nitrogen-doped TiO_2 modified zeolite in the degradation of Reactive Yellow 125 azo dye, *J. Taiwan Inst. Chem. Eng.,* 44(2013), 270-278.
13. R. Marandi, M. E. Olya, B. Vahid, M. Khosravi, and M. Hatami, Kinetic Modeling of Photocatalytic Degradation of an Azo Dye Using Nano-TiO_2/Polyester, *Environ. Eng. Sci.,* 29(2012), 957-963.
14. A. Aguedach, S. Brosillon, J. Morvan, and E. K. Lhadi, Influence of ionic strength in the adsorption and during photocatalysis of reactive black 5 azo dye on TiO_2 coated on non woven paper with SiO_2 as a binder, *J. Hazard. Mater.,* 150(2008), 250-256.
15. M. Vaez, A. Z. Moghaddam, N. M. Mahmoodi, and S. Alijani, Decolorization and degradation of acid dye with immobilized titania nanoparticles, *Process Saf. Environ. Prot.,* 90(2012), 56-64.
16. L. C. Juang, G. U. Semblante, S.-J. You, and S.-H. Hong, Degradation of 2-chlorophenol using carbon nanotube/titanium oxide composite prepared by hydrothermal method, *J Taiwan Inst Chem Eng,* 44(2013), 432-437.
17. W. C. Lin, W. D. Yang, and S. Y. Jheng, Photocatalytic degradation of dyes in water using porous nanocrystalline titanium dioxide, *J. Taiwan Inst. Chem. Eng.,* 43(2012), 269-274.
18. A. Eshaghi, M. Pakshir, and R. Mozaffarinia, Preparation and characterization of TiO_2 sol–gel modified nanocomposite films, *J. Sol-Gel Sci. Technol.,* 55(2010), 278-284.
19. A. Eshaghi, R. Mozaffarinia, M. Pakshir, and A. Eshaghi, Photocatalytic properties of TiO_2 sol-gel modified nanocomposite films, *Ceram. Int.,* 37(2011), 327-331.
20. N. Arconada, Y. Castro, and A. Durán,

Photocatalytic properties in aqueous solution of porous TiO_2-anatase films prepared by sol–gel process, *Appl. Catal., A,* 385(2010), 101-107.

21. Y. Zhao, X. Li, Q. Li, and C. Deng, Enhancement of the Photoelectric Performance of Dye-sensitized Solar Cells by Sol-gel Modified TiO_2 Films, *J. Mater. Sci. Technol.,* 27(2011), 764-768.
22. K. Sahel, N. Perol, F. Dappozze, M. Bouhent, Z. Derriche, and C. Guillard, Photocatalytic degradation of a mixture of two anionic dyes: Procion Red MX-5B and Remazol Black 5 (RB5), *J. Photochem. Photobiol., A,* 212(2010), 107-112.
23. J. Yu and B. Wang, Effect of calcination temperature on morphology and photoelectrochemical properties of anodized titanium dioxide nanotube arrays, *Appl. Catal., B,* 94(2010), 295-302.
24. L. Caballero, K. A. Whitehead, N. S. Allen, and J. Verran, Inactivation of Escherichia coli on immobilized TiO_2 using fluorescent light, *J. Photochem. Photobiol., A,* 202(2009), 92-98.
25. A. Fujishima, X. Zhang, and D. A. Tryk, TiO_2 photocatalysis and related surface phenomena, *Surf. Sci. Rep.,* 63(2008), 515-582.
26. A. R. Khataee, M. Zarei, M. Fathinia, and M. K. Jafari, Photocatalytic degradation of an anthraquinone dye on immobilized TiO_2 nanoparticles in a rectangular reactor: Destruction pathway and response surface approach, *Desalination,* 268(2011), 126-133.
27. W. Bahnemann, M. Muneer, and M. M. Haque, Titanium dioxide-mediated photocatalysed degradation of few selected organic pollutants in aqueous suspensions, *Catal. Today,* 124(2007), 133-148.
28. M. A. Behnajady, N. Modirshahla, N. Daneshvar, and M. Rabbani, Photocatalytic degradation of an azo dye in a tubular continuous-flow photoreactor with immobilized TiO_2 on glass plates, *Chem Eng J,* 127(2007), 167-176.
29. N. M. Mahmoodi, M. Arami, N. Y. Limaee, and N. S. Tabrizi, Decolorization and aromatic ring degradation kinetics of Direct Red 80 by UV oxidation in the presence of hydrogen peroxide utilizing TiO_2 as a photocatalyst, *Chem. Eng. J.* 112(2005), 191-196.
30. J. Saien and A. R. Soleymani, Degradation and mineralization of Direct Blue 71 in a circulating upflow reactor by UV/TiO_2 process and employing a new method in kinetic study, *J. Hazard. Mater.,* 144(2007), 506-512.
31. Z. Sun, Y. Chen, Q. Ke, Y. Yang, and J. Yuan, Photocatalytic degradation of a cationic azo dye by TiO_2/bentonite nanocomposite, *J. Photochem. Photobiol., A,* 149(2002), 169-174.
32. Y. Chen, Z. Sun, Y. Yang, and Q. Ke, Heterogeneous photocatalytic oxidation of polyvinyl alcohol in water, *J. Photochem. Photobiol., A,* 142(2001), 85-89.
33. G. Al-Sayyed, J. C. D'Oliveira, and P. Pichat, Semiconductor-sensitized photodegradation of 4-chlorophenol in water, *J. Photochem. Photobiol., A,* 58(1991), 99-114.
34. Y. Jiang, Y. Sun, H. Liu, F. Zhu, and H. Yin, Solar photocatalytic decolorization of C.I. Basic Blue 41 in an aqueous suspension of TiO_2-ZnO, *Dyes Pigmnts.,* 78(2008), 77-83.
35. E. Stathatos, D. Papoulis, C. A. Aggelopoulos, D. Panagiotaras, and A. Nikolopoulou, TiO_2/palygorskite composite nanocrystalline films prepared by surfactant templating route: Synergistic effect to the photocatalytic degradation of an azo-dye in water, *J. Hazard. Mater.,* 211-212(2012), 68-76.